Available online at www.sciencedirect.com
SCIENCE DIRECT®
ELSEVIER
International Journal of Solids and Structures 41 (2004) 7471–7492
INTERNATIONAL JOURNAL OF SOLIDS and STRUCTURES
www.elsevier.com/locate/ijsolstr

A numerical simulation for effective elastic moduli of plates with various distributions and sizes of cracks

Lianxi Shen, Jackie Li *

Department of Mechanical Engineering, City College of New York, CUNY 140th Street and Convent Ave., New York, NY 10031, USA

Received 1 July 2003; received in revised form 11 February 2004
Available online 6 August 2004

Abstract

A fast convergent numerical model is developed to calculate the effective moduli of plates with various distributions and sizes of cracks, in which the crack line is divided into M parts to obtain the unknown traction on the crack line. When $M = 1$, the model reduces to Kachanov's approximation method [Int. J. Solids Struct. 23 (1987) 23]. Six types of crack distributions and three kinds of crack sizes are considered, which are four regular (equilateral triangle, equilateral hexagon, rectangle, and diamond) and two random distributions (random location and orientation, and parallel orientation and random location), and one, two and random crack sizes. Some typical examples are also analyzed using the finite element method (FEM) to validate the present model. Then, the effective moduli associated with the crack distributions and sizes are calculated in detail. The present results for the regular distributions show some very interesting phenomena that have not been revealed before. And for the two random distributions, as the effective moduli depend on samples due to the randomness, the effect of the sample size and number are analyzed first. Then, effective moduli for plates with the three sizes of cracks are calculated. It is found that the effect of crack sizes on the effective moduli is significant for high crack densities, and small for low crack densities, and the random crack size leads to the lowest effective moduli. The present numerical results are compared with several popular micromechanics models to determine which one can provide the optimum estimation of the effective moduli of cracked plates with general crack densities. Furthermore, some existing numerical results are analyzed and discussed.

Keywords: Effective moduli; Regular and random distributions of cracks; Crack size effect; Sample size and number; Numerical model

1. Introduction

The effective elastic moduli of heterogeneous materials have been extensively studied in the past decades. The well-known micromechanics models include the non-interacting solution, the self-consistent method (e.g. Hill, 1965; Budiansky and O'Connell, 1976; Hoenig, 1979; Laws and Brockenbrough, 1987; Laws and Dvorak, 1987), the generalized self-consistent method (e.g. Christensen and Lo, 1979; Huang et al., 1994),

* Corresponding author. Tel.: +1-212-650-5207; fax: +1-212-650-8013.
E-mail address: j.li@ccny.cuny.ed (J. Li).

0020-7683/$ - see front matter © 2004 Elsevier Ltd. All rights reserved.
doi:10.1016/j.ijsolstr.2004.02.016

the differential method (e.g., Salganik, 1973; Norris, 1985; Zimmerman, 1985, 1991; Hashin, 1988), and the Mori–Tanaka method (Mori and Tanaka, 1973; Weng, 1984, 1990), among others. For cracked solids, the Mori–Tanaka method coincides with the non-interacting solution (Benveniste, 1986). These micromechanics models usually simplify the complex geometry of the matrix with randomly distributed inhomogeneities into the problem of a homogeneous media with only one inhomogeneity. The micromechanics models have been reviewed by many researchers, such as Willis (1981), Hashin (1983), Christensen (1990), Nemat-Nasser and Hori (1993), and Kachanov (1992, 1994). In general, the effective moduli lie between the predictions of the Mori–Tanaka method and the differential method. To assess the validity of these models, some numerical calculations were recently carried out, which considered the mutual positions among many spherical inhomogeneities or cracks. In the present study, cracked solids are considered.

For three-dimensional cracked solids, numerical calculations have not been reported. And for two-dimensional cracked solids, several numerical results have been published where approximate numerical models or boundary element methods were used to analyze some samples with many random cracks. It is expected that the results for the 2-D case may be an indicator to understand the 3-D case. However, these existing numerical results are not agreeable with each other for crack densities higher than 0.3.

Kachanov (1987) proposed a simple approximate method to analyze the problem of an infinite matrix with a finite number of cracks, and derived expressions of effective moduli of solids with cracks that can consider the mutual positions of cracks within a square sample. Then, Kachanov (1992) did a numerical calculation for effective Young's moduli of 2-D solids with random or parallel cracks. This is also the first numerical calculation of effective moduli that accounts for the mutual positions of many cracks, such as 25 cracks in his calculation. The results are slightly higher than the predictions of the non-interacting solution. Huang et al. (1994) pointed out that Kachanov's numerical results actually neglected the interaction between cracks outside and inside the square sample based on the concept of an infinite cracked solid consisting of doubly periodic blocks. They proposed an approximate method to improve the problem, in which an extra layer of cracked solid with 200 cracks is added around the initial square sample with 25 cracks, and calculated 15 samples to get the effective bulk modulus of solids with random cracks for crack density up to about 0.5. Their results are close to the prediction of the generalized self-consistent method for high crack densities. Furthermore, Huang et al. (1996) provided another numerical method to analyze an infinite doubly periodic 2-D solid, in which the boundary element method was used to analyze a square unit cell containing 25 randomly distributed cracks. Fifteen samples with random or parallel cracks for each crack density of 0.1, 0.2, 0.4, and 0.6 were calculated. For random cracks, as the crack density increases, their results vary from close to the differential method to close to the generalized self-consistent method. For parallel cracks, their effective Young's moduli keep the same trend, but their effective shear moduli are agreeable with the differential method until crack density of 0.6. Renaud et al. (1996) proposed a boundary element method to analyze 2-D cracked solids, which they called the displacement discontinuity method. They calculated a rectangular cracked plate for each crack density up to about 0.3. The effective Young's modulus was taken as the mean value of the two computations done in the horizontal and vertical directions. They also analyzed the case of random sizes of cracks varying between 1 and 10. Their results are agreeable with the differential method, and the crack size effect is small. Zhan et al. (1999) proposed a numerical method to analyze a finite plate with multiple cracks. They calculated 15 finite square samples with 36 random or parallel cracks for each crack density from 0.1 to 0.35 to get the effective Young's moduli. Their results are close to the differential method for crack density up to 0.3 and become significant higher than the differential method for 0.35. Shen and Yi (2000a,b, 2001) proposed a new energy balance equation, which exactly relates the effective moduli to the strain energy change of an infinite body due to the presence of a finite number of inhomogeneities in a circular or spherical region. The problem indicated by Huang et al. (1994) was simply and exactly solved using this energy approach. Then, they calculated the effective moduli by combining the approximate method (Kachanov, 1987) and their energy balance equation. Fifty random cracks and 200 parallel cracks were considered in their calculations for crack

density up to 0.6 (Shen and Yi, 2000b, 2001). Their results are close to those of Huang et al. (1996). Feng et al. (2003) calculated effective Young's moduli associated with random and parallel cracks up to crack density of 1 based on the combination of the effective stress field approach and Kachanov's method (Kachanov, 1987). Their results for the random cracks lie between the non-interaction solution and the differential method, but closer to the latter. And for the parallel cracks, their results are agreeable with the differential method (Hashin, 1988).

It can be seen that these existing numerical results support the differential method for crack density less than 0.3. But as the crack density increases from 0.3 to 0.6, these numerical results vary between the differential method and the non-interacting solution. So it is not easy to assess which one is more accurate for the case of high crack density. Actually, approximations and/or insufficiently large sample are involved in the existing results. For example, the model by Huang et al. (1994) involves the assumption that the interaction between cracks outside and inside a square sample was approximated as the interaction between the cracks in a layer of cracked materials and the cracks inside the square sample. And the model by Shen and Yi (2000b, 2001) adopted the approximate method by Kachanov (1987). The model by Feng et al. (2003) adopted both the approximate method by Kachanov (1987) and an approximate effective far-field stress. The validity of these approximations was not verified. The methods by Huang et al. (1996), Renaud et al. (1996), and Zhan et al. (1999) do not involve assumptions, and should lead to agreeable results. One possible reason for their discrepancies is that the sample size and/or number of cracks used are not sufficient for the effective moduli to stabilize. Therefore, a careful and thorough study is of great interest for the researchers in the field.

One of the purposes of the present paper is to complete this task, and the other is to investigate the effect of crack distributions and sizes. It is noted that the focus of the present study is on the effective moduli, even though the developed method is identically valid for the analysis of stress fields including intensity factors.

An outline of the paper is as follows. In Section 2, a formulation for the effective moduli is derived, which includes a system of integral equations controlling the effective moduli, and a numerical method for accurately solving the system of integral equations. In Section 3, plates with the four regular distributions of cracks are calculated for one and two sizes of cracks. Some very interesting phenomena are revealed. For example, the effective moduli do not gradually decrease to zero, but abruptly drop to zero in a very narrow region near the maximum crack length. And the effective Young's modulus becomes much larger, but the effective shear one gets a little smaller due to the crack size effect for the rectangular distribution. In Section 4, plates with the two randomly distributed cracks are analyzed. The three crack sizes are considered. The sample number and size at which the effective moduli can stabilize are analyzed first, and then the effective moduli for the two random distributions with crack density up to 0.6 are numerically obtained. And in Section 5, theoretical aspects of the effective moduli are analyzed, including the exact and explicit dependence of the effective moduli on the matrix Poisson's ratio and a summary of existing micromechanics models and their comparison with the present and existing numerical results. Finally, a brief conclusion of the present study is given in Section 6.

2. Formulation

2.1. Governing equations of effective moduli

2-D plane stress problems of cracked plates are considered in the study. Fig. 1(a) and (b) show a circular sample of a cracked plate and a homogeneous circular plate with the same size that are embedded in an infinite matrix, respectively. The infinite matrix is subjected to a uniform far-field stress tensor $\boldsymbol{\sigma}^{\infty}$. Let Δf_{micro} and $\Delta f_{\text{effective}}$ denote the strain energy changes of the infinite matrix due to the presence of the

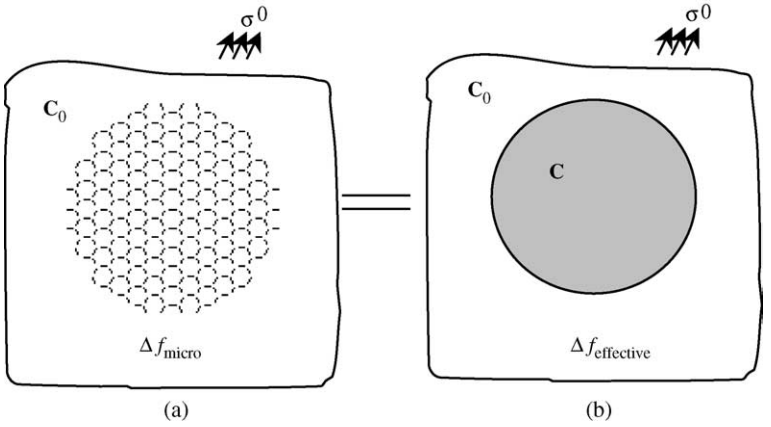

Fig. 1. Schematic diagram for the energy balance equation that relates the effective moduli of cracked plates to the problem of an infinite matrix with a finite number cracks in a circular sub-region.

circular sample and the homogeneous circular plate. The unknown elastic moduli of the homogeneous circular plate are defined as the effective elastic moduli of the cracked plate through the equality as follows:

$$\Delta f_{\text{effective}} = \Delta f_{\text{micro}}. \tag{1}$$

It is clear that if the circular sample is so large that the statistically uniform condition can be assumed, the present definition is equivalent to the conventional one. It is noted that the equality was used as an assumption by Shen and Yi (2000a,b, 2001). It can be easily seen that the circular sample does not have to be circular, but the circular shape is the most convenient. Also, it should be mentioned that the configuration of an infinite matrix containing a sample was assumed by Ju and Chen (1994), Nemat-Nasser and Hori (1995), Ponte Castañeda and Willis (1995), Zheng and Du (2001) and Feng et al. (2003) directly or indirectly. The novel aspect of the model by Shen and Yi (2000a,b, 2001) is that they skillfully assumed the effective configuration of an infinite matrix containing a homogeneous sample. This simply relates the effective moduli to the problem of an infinite matrix containing a finite number of inhomogeneities.

When the materials of the infinite matrix and plate matrix are assumed identical, Fig. 1(a) becomes the problem of an infinite matrix containing N cracks. It is well-known that the strain energy change Δf_{micro} can be expressed in terms of the unknown displacement discontinuities $\boldsymbol{b}_i$ of the N cracks across the crack lines l_i as follow:

$$\Delta f_{\text{micro}} = \frac{1}{2}\boldsymbol{\sigma}^{\infty} : \sum_{i=1}^{N} \int_{-l_i}^{l_i} \frac{1}{2}(\boldsymbol{n}_i \boldsymbol{b}_i(\varsigma_i) + \boldsymbol{b}_i(\varsigma_i)\boldsymbol{n}_i)\,\mathrm{d}\varsigma_i, \tag{2}$$

where $\boldsymbol{n}_i$ is a unit vector normal to the ith crack line, and $[-l_i, l_i]$ is the region of the ith crack. As the unit vector normal to the ith crack line $\boldsymbol{n}_i$ is constant, (2) can be further reduced as

$$\Delta f_{\text{micro}} = \frac{1}{2}\boldsymbol{\sigma}^{\infty} : \sum_{i=1}^{N} \frac{1}{4l_i}[\boldsymbol{n}_i\langle \boldsymbol{b}_i\rangle + \langle \boldsymbol{b}_i\rangle \boldsymbol{n}_i], \tag{3}$$

where $\langle \boldsymbol{b}_i\rangle = \frac{1}{2l_i}\int_{-l_i}^{l_i} \boldsymbol{b}_i(\varsigma_i)\,\mathrm{d}\varsigma_i$ is the average displacement discontinuity of the ith crack.

Fig. 1(b) is the problem of an infinite matrix containing a homogeneous circular inclusion. The strain energy change $\Delta f_{\text{effective}}$ can be obtained according to Eshelby's method (Eshelby, 1957):

$$\Delta f_{\text{effective}} = -\frac{1}{2}A\boldsymbol{\sigma}^{\infty} : [\boldsymbol{C}_0 : (\boldsymbol{C} - \boldsymbol{C}_0)^{-1} : \boldsymbol{C}_0 + \boldsymbol{C}_0 : \boldsymbol{S}_0]^{-1} : \boldsymbol{\sigma}^{\infty}, \tag{4}$$

where $\boldsymbol{C}$ and $\boldsymbol{C}_0$ are the effective elastic stiffness tensor of the cracked plate and elastic stiffness tensor of the plate matrix, A denotes the area of the circular sample, which also represents the corresponding sub-region in terms of the context, and $\boldsymbol{S}_0$ is 2-D Eshelby's tensor associated with Poisson's ratio of the matrix and a circular shape. Substituting (3) and (4) into (1) leads to the particular form as follows

$$\boldsymbol{\sigma}^{\infty} : [\boldsymbol{C}_0 : (\boldsymbol{C} - \boldsymbol{C}_0)^{-1} : \boldsymbol{C}_0 + \boldsymbol{C}_0 : \boldsymbol{S}_0]^{-1} : \boldsymbol{\sigma}^{\infty} = -\frac{1}{A}\boldsymbol{\sigma}^{\infty} : \sum_{i=1}^{N} \frac{1}{4l_i}[\boldsymbol{n}_i\langle \boldsymbol{b}_i\rangle + \langle \boldsymbol{b}_i\rangle \boldsymbol{n}_i]. \tag{5}$$

To find the unknown average displacement discontinuities $\langle \boldsymbol{b}_i\rangle$, the problem of the infinite matrix containing N cracks as shown in Fig. 1(a) needs to be solved, which can been represented as a superposition of N problems, each involving only one crack but loaded by unknown tractions $\boldsymbol{t}_i$. The tractions $\boldsymbol{t}_i$ are controlled by a system of integral equations (e.g. Kachanov, 1987):

$$\boldsymbol{t}_i(\varsigma_i) = \boldsymbol{t}_i^0 + \boldsymbol{n}_i \cdot \sum_{j\neq i} \int_{-l_j}^{l_j} \boldsymbol{\sigma}_j^n(\varsigma_i, \varsigma_j)[\boldsymbol{n}_j \cdot \boldsymbol{t}_j(\varsigma_j)] + \boldsymbol{\sigma}_j^{\tau}(\varsigma_i, \varsigma_j)[\boldsymbol{\tau}_j \cdot \boldsymbol{t}_j(\varsigma_j)]\,\mathrm{d}\varsigma_j, \tag{6}$$

where $\boldsymbol{t}_i^0 = \boldsymbol{n}_i \cdot \boldsymbol{\sigma}^{\infty}$, $\boldsymbol{n}_j$ and $\boldsymbol{\tau}_j$ are the unit normal and tangential vectors of the jth crack, and $\boldsymbol{\sigma}_j^n(\varsigma_i, \varsigma_j)$ and $\boldsymbol{\sigma}_j^{\tau}(\varsigma_i, \varsigma_j)$ are the stress tensors at a current point ς_i on the ith crack, generated by a pair of equal and opposite unit forces located at a current point ς_j and along normal and tangential directions on the jth crack. The fundamental solutions of one single crack problem, i.e., $\boldsymbol{\sigma}_j^n(\varsigma_i, \varsigma_j)$ and $\boldsymbol{\sigma}_j^{\tau}(\varsigma_i, \varsigma_j)$ are available (see Muskhelishvili, 1963). Then, using the solution of the average displacement discontinuity due to a pair of point forces located at ς_i (see Kachanov, 1994), $\langle \boldsymbol{b}_i\rangle$ can be linked with $\boldsymbol{t}_i$ based on the superposition principle as follows:

$$\langle \boldsymbol{b}_i\rangle = \frac{4l_i}{E_0} \int_{-l_i}^{l_i} \boldsymbol{t}_i(\varsigma_i)[1 - (\varsigma_i/l_i)^2]^{1/2}\,\mathrm{d}\varsigma_i, \tag{7}$$

where E_0 is the Young's modulus of the plate matrix. Therefore, (5)–(7) provide a system of equations rigorously governing the effective elastic moduli $\boldsymbol{C}$ of a cracked plate.

2.2. A fast convergent numerical method for the system of integral equations

Kachanov's approximate method simplifies the exact relations (6) and (7) as $\langle \boldsymbol{t}_i\rangle = \boldsymbol{t}_i^0 + \sum_{k\neq i} \boldsymbol{\Lambda}_{ik} \cdot \langle \boldsymbol{t}_k\rangle$ and $\langle \boldsymbol{b}_i\rangle = \frac{\pi l_i}{E_0}\langle \boldsymbol{t}_i\rangle$ (Kachanov, 1987). This approximate method is involved in the numerical results by Shen and Yi (2000b, 2001) and Feng et al. (2003). As the existing numerical results do not agree with each other, it is necessary to check the accuracy of the approximate method. Therefore, several problems of an infinite matrix containing 20 cracks in a circular sub-region are preliminarily analyzed using FEM and the approximate method. The 20 cracks may be regularly or randomly distributed. The various crack densities of the 20 cracks in the circular sub-region are considered. The comparisons show that when the cracks are randomly distributed and crack density is not low, the approximate method may cause significant errors, but when the cracks are regularly distributed, the errors caused by the approximate method is small. Fig. 2(a) and (b) show two examples of 20 random and parallel cracks in a circular region with crack density of 0.4 and 0.6, respectively. The strain energy changes $\Delta f_{\mathrm{micro}}$ of an infinite matrix due to the presence of these cracks are obtained using the approximate method and FEM, which is relevant to the effective moduli. For the random cracks, hydrostatic and pure shear far-field stresses are applied, and for the parallel cracks, simple pull and pure shear far-field stresses are taken. For the FEM analysis, a sufficiently large square matrix is used to replace the infinite matrix. After normalized by the corresponding ones using the non-interacting approximation, the results of the strain energy changes $\Delta f_{\mathrm{micro}}$ based on the approximate method are 0.648 and 0.861 for the random cracks, and 0.417 and 0.739 for the parallel cracks, while the corresponding results using FEM are 0.731 and 1.05 for the random cracks, and 0.477 and 0.929 for the

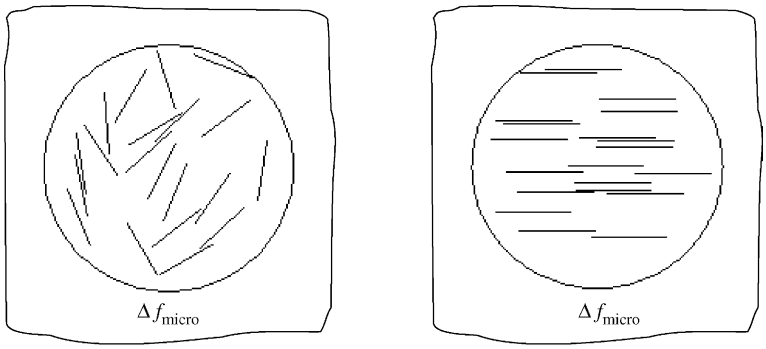

Fig. 2. Two examples of an infinite matrix with 20 random or parallel cracks in a circular sub-region, where the strain energy changes Δf_{micro} are solved using FEM to check the validity of the approximate method by Kachanov (1987).

parallel cracks. It is seen that the relative differences are about 10–20%. As a large number of calculations for much more cracks are needed to get the effective moduli, a fast convergent numerical method is developed here.

Equally dividing the region $[-l_i, l_i]$ associated with the ith crack into M parts, and letting $\bar{\boldsymbol{t}}_i(\zeta_p)$ be the average value of the unknown traction $\boldsymbol{t}_i(\varsigma_i)$ over the pth sub-region $[\zeta_p, \zeta_{p+1}]$ with $p = 1, 2, \ldots, M$, then using $\bar{\boldsymbol{t}}_i(\zeta_p)$ to replace $\boldsymbol{t}_i(\varsigma_i)$ in the right side of (6), it becomes

$$\boldsymbol{t}_i(\varsigma_i) = \boldsymbol{t}_i^0 + \boldsymbol{n}_i \cdot \sum_{j\neq i} \sum_{p=1}^{M} \int_{\zeta_p}^{\zeta_{p+1}} \boldsymbol{\sigma}_j^n(\varsigma_i, \varsigma_j)\boldsymbol{n}_j + \boldsymbol{\sigma}_j^\tau(\varsigma_i, \varsigma_j)\boldsymbol{\tau}_j \, \mathrm{d}\varsigma_j \cdot \bar{\boldsymbol{t}}_i(\varsigma_p). \tag{8}$$

Averaging the two sides of (8) over the qth sub-region $[\zeta_q, \zeta_{q+1}]$ $(q = 1, 2, \ldots, M)$ leads to

$$\bar{\boldsymbol{t}}_i(\zeta_q) = t_i^0 + \sum_{j\neq i} \sum_{p=0}^{M} \mathbf{D}_{iq}^{jp} \cdot \bar{\boldsymbol{t}}_j(\zeta_p) \tag{9}$$

with

$$\mathbf{D}_{iq}^{jp} = \frac{1}{\zeta_{q+1} - \zeta_q} \int_{\zeta_q}^{\zeta_{q+1}} \int_{\zeta_p}^{\zeta_{p+1}} \boldsymbol{n}_i \cdot [\boldsymbol{\sigma}_j^n(\zeta_i, \zeta_j)\boldsymbol{n}_j + \boldsymbol{\sigma}_j^\tau(\zeta_i, \zeta_j)\boldsymbol{\tau}_j] \, \mathrm{d}\zeta_j \, \mathrm{d}\zeta_i. \tag{10}$$

Eq. (9) is a set of $N \times M$ vectorial linear algebraic equations for $\bar{\boldsymbol{t}}_i(\zeta_p)$. After solving $\bar{\boldsymbol{t}}_i(\zeta_p)$, $\boldsymbol{t}_i(\varsigma_i)$ can be obtained from (8). It is noted that when taking $M = 1$, the numerical method reduces to the approximate method for $\boldsymbol{t}_i(\varsigma_i)$ by Kachanov (1987). So, the present method can be thought as an extension of Kachanov's method. The feature of the method is that it carries out an iterate operation by taking $\bar{\boldsymbol{t}}_i(\zeta_p)$ as initial values. The problem of two collinear cracks is similarly taken as an example to show the convergent rate of the numerical method. The two cracks occupy the regions $[-k, -1]$ and $[k, 1]$ on x axis following Kachanov (1987). The stress intensities of the inner tip at locations $-k$ or k are shown in Table 1 for various crack spaces. It is seen that for $M = 1$, the results of Kachanov (1987) are recovered, and when k is very small, such as 0.005, the subdivision $M = 5$ is enough to make the relative error less than 1%. So the numerical method of (8) and (9) has a very fast convergent rate. Also, the strain energy changes of two examples shown in Fig. 2(a) and (b) are analyzed using the present numerical model of (3), (7)–(9). It is found that the results based on subdivision $M = 5$ are agreeable with FEM calculations.

Table 1
Normalized stress intensity factor $K_I(k)/K_I^0$ at the inner tip

Crack space k	$K_I(k)/K_I^0$ using various subdivision number M					Accurate
	1	2	3	4	5	
0.2	1.1120	1.1126	1.1126	1.1126	1.1126	1.1125
0.1	1.2510	1.2558	1.2561	1.2560	1.2558	1.2551
0.05	1.4525	1.4726	1.4758	1.4763	1.4761	1.4729
0.02	1.8085	1.8835	1.9046	1.9122	1.9151	1.9046
0.01	2.1337	2.2870	2.3423	2.3681	2.3813	2.3716
0.005	2.4936	2.7594	2.8739	2.9362	2.9736	2.9992

2.3. The procedure to numerically calculate effective moduli of a sample

Eqs. (5), (7)–(9) form an accurate numerical model to obtain the effective moduli. Two special types of cracked plates are particularly of concern in the study. The first one is associated with isotropic properties where the effective elastic stiffness tensor $\boldsymbol{C}$ can be characterized by the bulk and shear moduli K and G. As shown in Fig. 3(a), (b) and (e), the random, equilateral triangular, and equilateral hexagonal distributions correspond to this case. The second is associated with a special orthotropic property. As shown in Fig. 3(c), (d) and (f), the parallel, diamond, and rectangular distributions correspond to the second case, where the effective elastic stiffness tensor $\boldsymbol{C}$ can be characterized by the Young's modulus normal to the crack direction and shear modulus along the crack direction, i.e., E_1 and G_{12}.

By applying the four far-field stress conditions, i.e., hydrostatic stress, pure shear, single pull, and pure shear with magnitudes σ_K^∞, σ_G^∞, σ_E^∞, and σ_G^∞, respectively, the four effective moduli K, G, E_1 and G_{12} can be independently calculated by taking advantage of the independent forms of (5) as follows

$$\frac{1}{K_0}\frac{K-K_0}{K_0+\xi(K-K_0)} = -\frac{1}{(\sigma_K^\infty)^2}\frac{1}{A}\boldsymbol{\sigma}_K^\infty : \sum_{i=1}^{N}\frac{1}{4l_i}[\boldsymbol{n}_i\langle\boldsymbol{b}_i\rangle + \langle\boldsymbol{b}_i\rangle\boldsymbol{n}_i], \tag{11}$$

$$\frac{1}{G_0}\frac{G-G_0}{G_0+\eta(G-G_0)} = -\frac{1}{(\sigma_G^\infty)^2}\frac{1}{A}\boldsymbol{\sigma}_G^\infty : \sum_{i=1}^{N}\frac{1}{4l_i}[\boldsymbol{n}_i\langle\boldsymbol{b}_i\rangle + \langle\boldsymbol{b}_i\rangle\boldsymbol{n}_i], \tag{12}$$

$$\frac{1}{E_0}\frac{E_1-E_0}{E_0+\xi_E(E-E_0)} = -\frac{1}{(\sigma_E^\infty)^2}\frac{1}{A}\boldsymbol{\sigma}_E^\infty : \sum_{i=1}^{N}\frac{1}{4l_i}[\boldsymbol{n}_i\langle\boldsymbol{b}_i\rangle + \langle\boldsymbol{b}_i\rangle\boldsymbol{n}_i], \tag{13}$$

$$\frac{1}{G_0}\frac{G_{12}-G_0}{G_0+\eta_G(G_{12}-G_0)} = -\frac{1}{(\sigma_G^\infty)^2}\frac{1}{A}\boldsymbol{\sigma}_G^\infty : \sum_{i=1}^{N}\frac{1}{4l_i}[\boldsymbol{n}_i\langle\boldsymbol{b}_i\rangle + \langle\boldsymbol{b}_i\rangle\boldsymbol{n}_i], \tag{14}$$

where $\xi = (1+v_0)/2$, $\eta = (3-v_0)/4$, $\xi_E = 5/8$, $\eta_G = (3-v_0)/4$, E_0 and v_0 denote Young's modulus and Poisson's ratio of the isotropic plate matrix, and K_0 and G_0 are 2-D bulk and shear moduli with $K_0/E_0/2(1-v_0)$ and $G_0 = E_0/2(1+v_0)$. The procedure to solve the effective modulus of a sample can be described as follows:

(a) produce a sample containing N cracks;
(b) apply a far-field stress condition correspondingly;
(c) select an initial number of M, say 5;
(d) solve the system of $N \times M$ vectorial linear algebraic equations (9) to get $\bar{t}_i(\zeta_p)$;
(e) substitute the $\bar{t}_i(\zeta_p)$ into (8) to get $\boldsymbol{t}_i(\varsigma_i)$ and then (7) to get $\langle\boldsymbol{b}_i\rangle$;

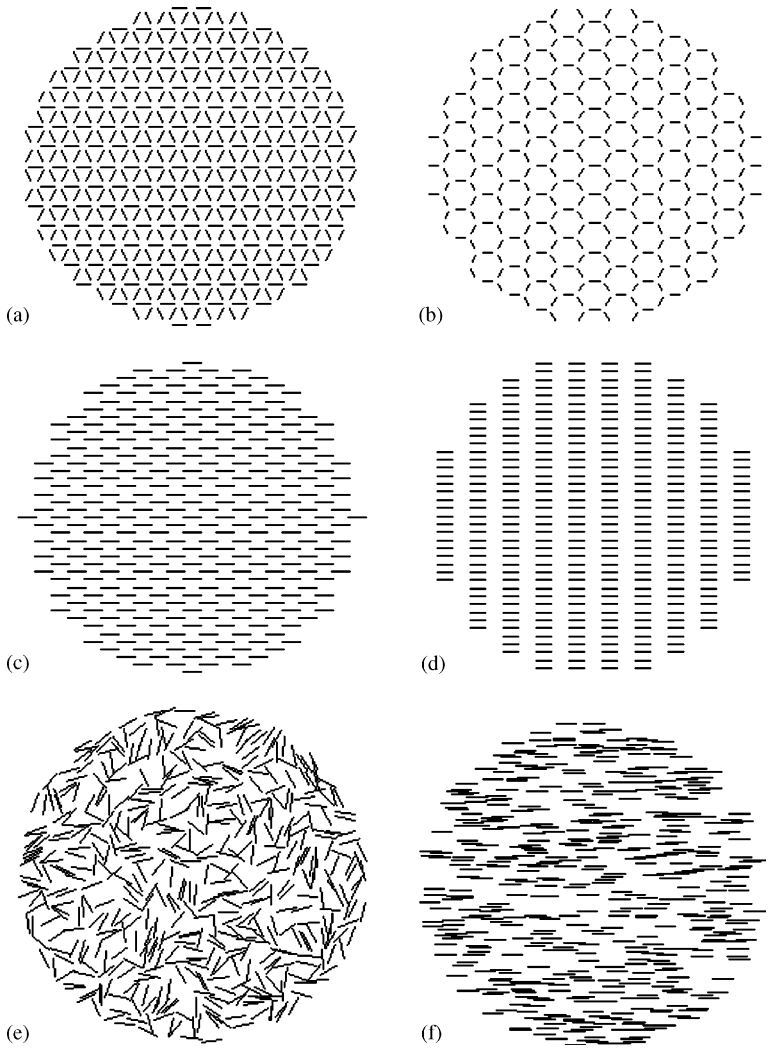

Fig. 3. The six types of distributions of cracks: (a) equilateral triangular, (b) equilateral hexagonal, (c) diamond, (d) rectangular, (e) random, and (f) parallel distributions.

(f) substitute the $\langle \boldsymbol{b}_i \rangle$ into the corresponding one of (11)–(14) to get an effective modulus of the sample;
(g) double the number M and return to (d), then go ahead to (f) to get another effective modulus of the sample;
(h) if the relative difference of the two effective moduli is less than 0.01, the later one is taken as the effective modulus of the sample, and the computation for the sample is stopped, otherwise return to (g).

For regular distributions of cracks, the effective moduli based on the procedure depend on the sample size characterized by the crack number N. When the number N is sufficiently large, the effective moduli stabilize. For random distributions of cracks, the computed effective moduli depend on the sample size and sample number. When the crack number N and the sample number are sufficiently large, the effective moduli stabilize. The determination of the crack number N and the sample number is given in the following

sections. Poisson's ratio of the plate matrix is taken to be zero for simplicity. It will be shown that the results with other Poisson's ratios can be exactly related to the results with Poisson's ratio being zero. This will be illustrated in Section 5.

3. Plates with regularly distributed cracks

3.1. Sample sizes

The crack density of a cracked plate is denoted as ρ, which is defined through a sufficiently large piece of the cracked plate as follows,

$$\rho = \frac{1}{A}\sum_{i=1}^{N} l_i^2, \tag{15}$$

where A, l_i and N are the area of the piece, the half length of the ith crack and the number of cracks included in the piece. For regular distributions, the crack density can be obtained based on a unit cell. As shown in Fig. 3(a)–(d), the circular samples of plates with the four distributions of cracks are considered in this study, which are the equilateral triangular, equilateral hexagonal, diamond, and rectangular distributions. Their crack densities can be obtained as $2\sqrt{3}l^2$, $2\sqrt{3}/3l^2$, l^2/d, and l^2/d, respectively, where l denotes the half crack length, d is the distance between two crack rows for the diamond and rectangular distributions, and the maximum crack length is taken as one unit. The circular samples are taken from a large cracked plate by drawing a circle with a symmetric point as center and the length with some units as radius. The circular samples contain those cracks only if their centers are inside the circle. The crack densities of the circular samples based on (15) are different from those based on a unit cell. But as the sample size increases, their difference approaches to zero.

As mentioned previously, the effective moduli vary with the sample size. The sample size can be characterized by the crack number in the sample. Following the calculation procedure listed in Section 2.3, the effective moduli are obtained for various sample sizes. It is found that the effective moduli can only stabilize (compared to larger sample sizes, their relative differences are less than 0.01) when the crack number is very large, say 500. The sample size with the number secures that the crack density based on (15) is agreeable with the one based on a unit cell.

Theoretically, when the sample size becomes sufficiently large, the displacement field in the sample is statistically uniform. So for the triangular and hexagonal distributions, the average displacement discontinuity $\langle \boldsymbol{b}_i \rangle$ should be the same for all the cracks for the far-field hydrostatic stress condition, and there are just two different values for all the average displacement discontinuity $\langle \boldsymbol{b}_i \rangle$ for the far-field pure shear condition, depending on the relative angles to the far-field shear stresses. For the diamond and rectangular distributions, the average displacement discontinuity $\langle \boldsymbol{b}_i \rangle$ should be the same for all the cracks under the simple pull and pure shear far-field stress condition. Actually, it is observed in calculation examples that the average displacement discontinuities of the cracks in the most outer layer are a little different from the inner cracks, and as the sample increases, the difference decreases. Also, a useful observation is that the average displacement discontinuities of the cracks in the center of the sample can stabilize at a small sample size. Therefore, taking the advantage, the effective moduli for regular distributions of cracks can be easily calculated based on relatively small samples.

3.2. Numerical results for the triangular and hexagonal distributions

Plates with these two distributions of cracks can be assumed isotropic due to the symmetry. Crack lengths from 0 to 0.99, which correspond to the crack densities from 0 to 0.8660 for the triangular

distribution and from 0 to 0.2887 for the hexagonal one are considered. The numerical results of the effective bulk and shear moduli are obtained following the calculation procedure. The effective moduli are also calculated using FEM to verify the present numerical model. These results are plotted in Fig. 4(a) and (b). It is seen that the present numerical model is agreeable with FEM results. As expected, the hexagonal distribution of cracks has much lower stiffness than the triangular one. Meanwhile, an interesting phenomenon is seen for the two distributions, in which the effective moduli can remain rather high when the crack length has reached 99% of its maximum length, which is called a boundary layer phenomenon.

Theoretically, the effective moduli must vanish at the maximum crack length. So they must drop to zero in the narrow region [0.99, 1] of crack length variation. Based on the analysis, the curves of the effective moduli corresponding to the crack length region [0.99, 1] are simply plotted by connecting the two end values of the effective moduli at 0.99 and 1. The effective moduli within the region are not calculated in detail due to the very slow convergence rate.

3.3. Numerical results for the diamond and rectangular distributions

Nemat-Nasser and Yu (1993) numerically calculated the effective moduli for the rectangular distribution with the crack row distance being 0.25 based on a unit cell containing one crack. To compare with their results, the crack row distance is also taken as 0.25 in the present calculation for the rectangular and diamond distributions. Hence, the maximum crack densities are 1 for the two distributions when the crack length reaches its maximum value 1. Similarly, the effective Young's and shear moduli are calculated for various crack lengths from 0 to 0.99 corresponding to crack density from 0 to 0.9801. The present results together with those of Nemat-Nasser and Yu (1993) are plotted in Fig. 5(a) and (b). It is noted that the results by Nemat-Nasser and Yu (1993) correspond to the case of plain strain problem with Poisson's ratio being 0.25. The results can be transformed to the present case, as illustrated in Section 5.

An interesting observation from the results in Fig. 5(a) and (b) is that, compared to the diamond distribution, the rectangular distribution has much higher effective Young's modulus, but lower effective shear modulus. Besides, it is seen that the present results are agreeable with those of Nemat-Nasser and Yu (1993) for all the crack densities except 1. Nemat-Nasser and Yu (1993) claimed that the effective Young's and

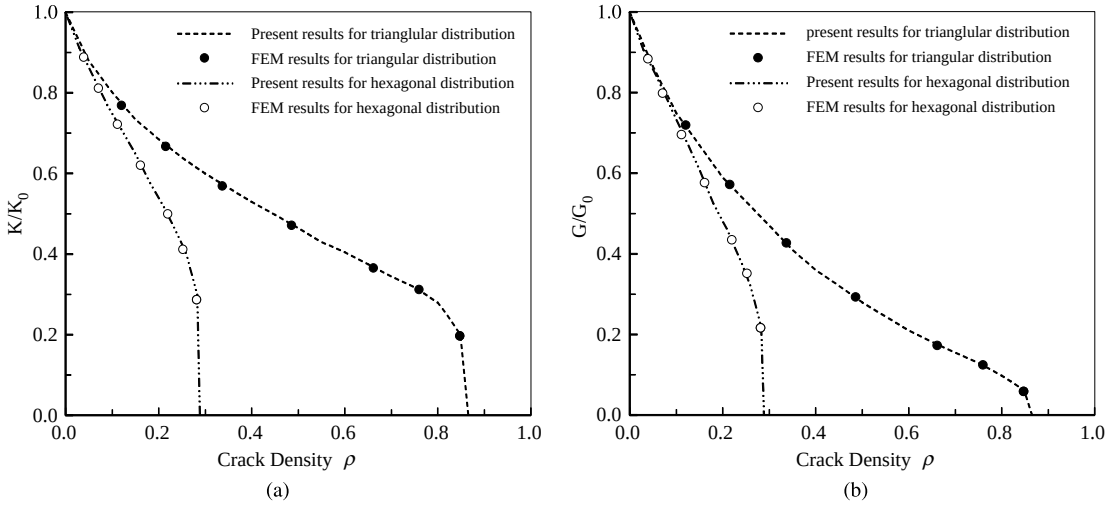

Fig. 4. The effective bulk and shear moduli of the equilateral triangular and hexagonal distributions based on the present model and finite element method (FEM).

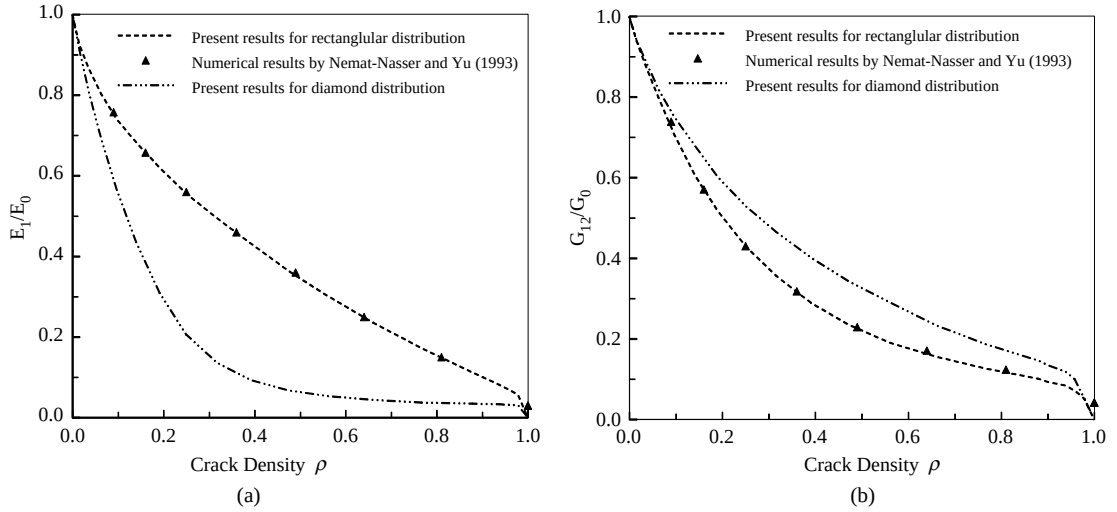

Fig. 5. The effective Young's and shear moduli of the diamond and rectangular distributions based on the present model and comparison with the numerical results of Nemat-Nasser and Yu (1993).

shear moduli were found to be about 0.03 and 0.05 at the maximum crack length 1. As the effective moduli must vanish at the crack length 1, they thought that the values of 0.03 and 0.05 might be the numerical error of their numerical model. However, as their model cannot be valid for the limit case of crack length 1, they had to get the values based on a limiting process of the crack length. It is assumed that the values of 0.03 and 0.05 were obtained using a crack length very close to 1, such as 0.999. As the boundary layer phenomenon similarly exists, the small values may accurately correspond to the effective moduli with the crack length 0.999.

Furthermore, the rectangle distribution with the same crack row distance being 0.25 is taken as an example to see the effect of crack size. Two sizes of cracks are considered. The big and small cracks are aligned column by column, and the distances between the crack centers keep the same as 1, as shown in Fig. 6. The three ratios of the big crack to the small one, i.e., 1, 5 and 10 are analyzed. The effective Young's and shear moduli versus crack density up to 0.6 are calculated and plotted in Fig. 6(a) and (b). It is interesting to see that compared to the case of one sized cracks, effective Young's modulus becomes much larger but effective shear modulus becomes a little smaller due to the crack size effect.

4. Plates with randomly distributed cracks

4.1. The generation of a sample

To generate a sample, a random number generator which randomly and successively generates the location of each crack is used to determine the centers of N cracks for parallel cracks, and the centers and orientations for random cracks in a circular region. When the location of a new crack is determined using one (the case of parallel cracks) or two (the case of random cracks) random numbers, the crack is checked if it overlaps with any of the previously generated cracks. If it overlaps with a previous crack, it needs to be regenerated using other random numbers. Deferent from the existing generation of cracks where the spacing between cracks is kept no smaller than 0.02 (Kachanov, 1992; Shen and Yi, 2001), the present calculation does not require the smallest spacing. The crack number, crack length and the radius of the

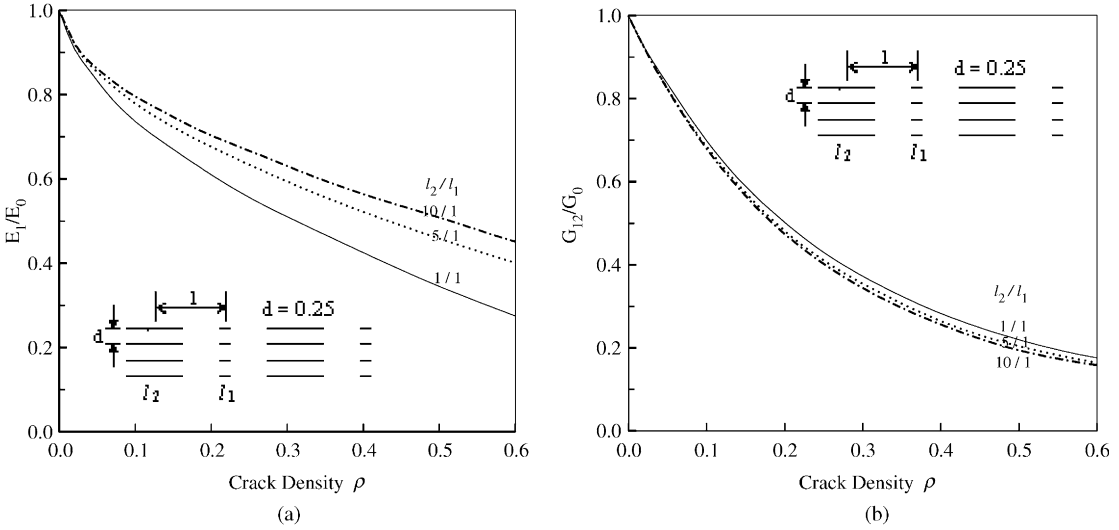

Fig. 6. The crack size effect on the effective moduli for the rectangular distribution.

circular region are given so that a crack density can be obtained. For two crack sizes, the big cracks are generated first. For random crack sizes, it is assumed that the crack sizes range from 1 to 10. A set of crack sizes are randomly determined first, and then the cracks with the crack sizes are randomly distributed in a circular region in the order from big to small cracks.

Once a sample is generated, its effective moduli can be calculated following the calculation procedure described in Section 2.3. However, for the random case, the effective moduli depend on samples. They can stabilize when sample size and number are sufficiently large. But how large a sample and how many samples for each sample size should be used to get the stabilized average value are not clear. Some existing calculations simply took 10 or 15 samples and 25, 36 or 50 cracks in each sample. However, the detailed analysis has not been done. Actually, those sample sizes are not sufficiently large, as shown in the following section.

4.2. Sample size and number at which effective moduli stabilize

The sample size and sample number at which the effective moduli can stabilize may vary with crack densities. So, the crack densities 0.1 and 0.6 are taken to carry out the study in details. The crack numbers from 50 to 500 and the sample numbers from 10 to 40 are considered. Figs. 7 and 8 plotted the results of effective moduli based on the various sample sizes. For each sample size, 20 samples are calculated. So, it is seen from these results that (a) the higher the crack density is, the larger the sample size that is required for the effective moduli to stabilize. For example, 50 and 300 cracks are suitable for crack density being 0.1 and 0.6; (b) The sample size has less effect on the effective shear modulus than on the bulk or Young's modulus for the high crack density 0.6; (c) for a sample size, the higher crack density shows a larger scatter of the effective moduli.

To check if 20 samples are sufficient for each sample size, the effect of sample number is analyzed. Fig. 9 shows the results of the effective bulk and Young's moduli for the random and parallel cracks with the crack density 0.6 and the sample size of 50 cracks. It is seen that 10–20 samples can be sufficient.

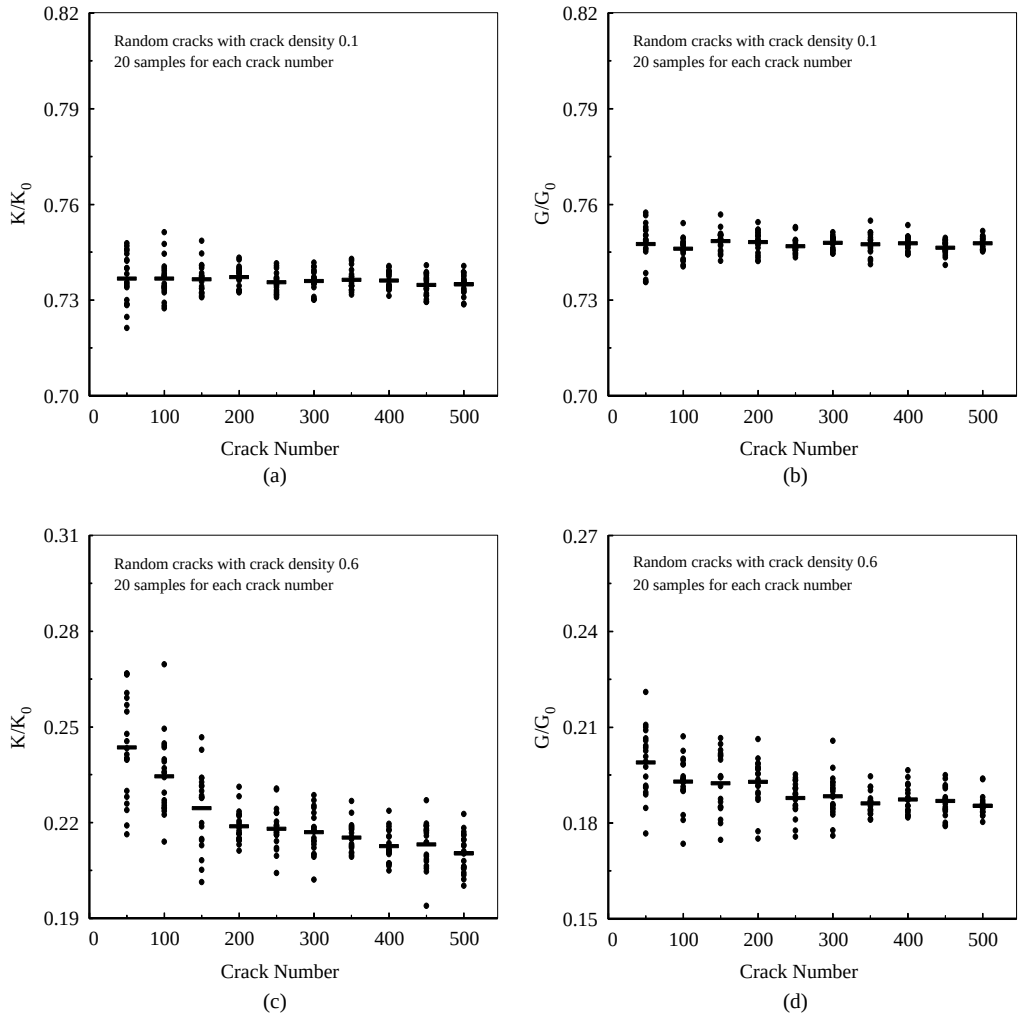

Fig. 7. The effect of sample size on the effective moduli for the random distribution of cracks with the low and high crack densities.

4.3. One, two and random sizes of cracks

Based on the analyses of the effect of sample size and number, 20 samples are taken for each case of the present calculations. For the one sized cracks, six sample sizes with crack number from 50 to 300 are taken for the six crack densities from 0.1 to 0.6. For the two sizes of cracks, the two ratios of the big and small cracks, i.e., 5 and 10 are considered. The crack densities of the big and small cracks are taken to be the same. So the number of the small cracks is 25 and 100 times as many as the big cracks for the two ratios of crack sizes. Therefore, 1300 cracks including 50 big cracks and 1250 small ones for the ratio 5, and 5050 cracks including 50 big cracks and 5000 small ones for the ratio 10 are considered in each sample. For the random sizes of cracks, the sample size of 2000 cracks is used. Then, the effective moduli of each sample are calculated following the calculation procedure. The average values are used to plot Fig. 10(a)–(d). It is seen that the crack size effect can decrease the effective moduli by about 10–30% for crack density 0.6. The effect

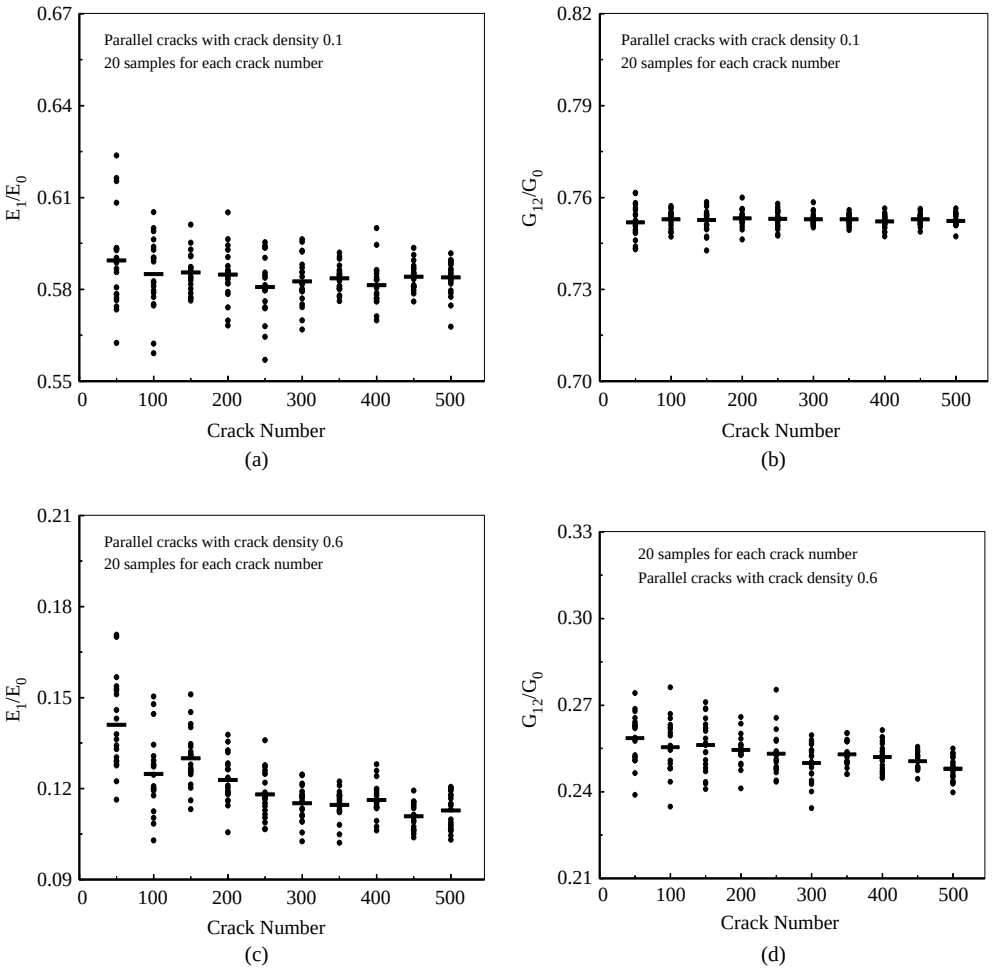

Fig. 8. The effect of sample size on the effective moduli for the parallel distribution of cracks with the low and high crack densities.

on the effective shear moduli is relatively less than that on the effective bulk and Young's moduli. In general, the effect of crack size can be significant for very high crack density, such as higher than 0.4.

5. Micromechanics analysis of effective moduli

5.1. Explicit and exact dependence of effective moduli on E_0 and v_0

Since the fundamental solutions $\boldsymbol{\sigma}_j^n(\varsigma_i,\varsigma_j)$ and $\boldsymbol{\sigma}_j^\tau(\varsigma_i,\varsigma_j)$ used in (6) are independent of Young's modulus E_0 and Poisson's ration v_0 of the plate matrix, it can be seen from (3), (6) and (7) that the strain energy change Δf_{micro} is independent of v_0 and is expressed as

$$\Delta f_{\text{micro}} = \frac{1}{E_0}\Delta f^0_{\text{micro}}, \tag{16}$$

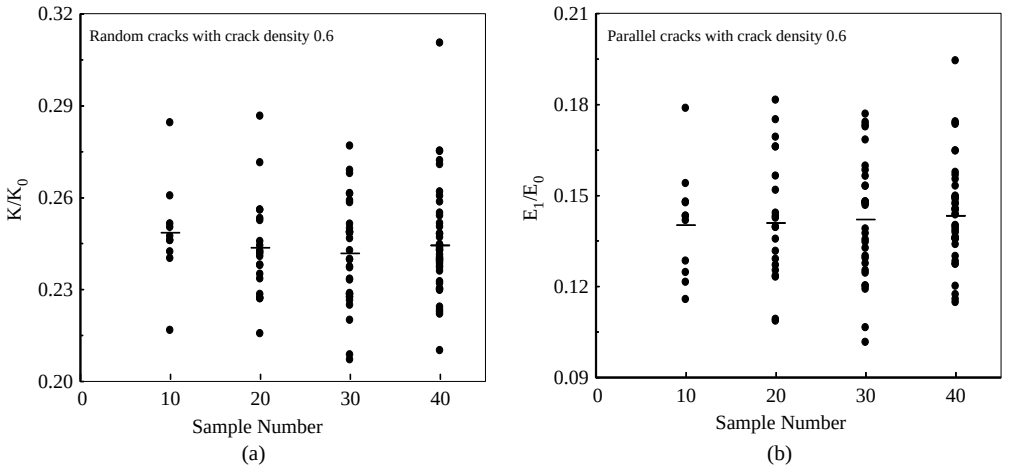

Fig. 9. The effect of sample number on the effective moduli for the random and parallel distributions of cracks with crack density 0.6.

where $\Delta f^0_{\text{micro}}$ is the strain energy change associated with a plate matrix with unit Young's modulus, which is also independent of v_0. By taking a unit area of circular sample, the right side of (11)–(14) can be expressed as $\frac{-2}{E_0}\Delta f^0_{\text{micro}}$ where $\Delta f^0_{\text{micro}}$ is only associated with the geometry information of the cracks contained in the circular samples and the types of the far-field stress conditions. Therefore, K and G, and E_1 and G_{12} can be derived as

$$\frac{K}{K_0} = 1 \Big/ \left(1 + \frac{1}{(1-v_0)} \frac{\Delta f^0_{\text{micro}}}{1 - \frac{1}{2}\Delta f^0_{\text{micro}}}\right), \tag{17}$$

$$\frac{G}{G_0} = 1 \Big/ \left(1 + \frac{1}{(1+v_0)} \frac{\Delta f^0_{\text{micro}}}{1 - \frac{1}{4}\Delta f^0_{\text{micro}}}\right), \tag{18}$$

$$\frac{E_1}{E_0} = 1 \Big/ \left(1 + \frac{2\Delta f^0_{\text{micro}}}{1 - \frac{3}{4}\Delta f^0_{\text{micro}}}\right), \tag{19}$$

$$\frac{G_{12}}{G_0} = 1 \Big/ \left(1 + \frac{1}{(1+v_0)} \frac{\Delta f^0_{\text{micro}}}{1 - \frac{1}{4}\Delta f^0_{\text{micro}}}\right). \tag{20}$$

It is noticed that $\Delta f^0_{\text{micro}}$ is dependent of the types of the far-field stress conditions and the geometry of cracks. So, $\Delta f^0_{\text{micro}}$ in the four expressions (17)–(20) may be different. It is known that Cherkaev et al. (1992) derived the stress invariance and shift characteristics of effective compliance in planar elasticity, which is also referred to as the CLM theorem. Zheng and Hwang (1996) derived more general shift characteristics of effective compliance for two-dimensional composites, and Hu and Weng (2001) gave a new derivative on the shift property, and obtained some new results for three-dimensional composites. For the current special case of cracks, the present expressions are agreeable with the shift characteristics of effective compliance by these researchers. But the present derivation is simple and direct, and the physical meaning of the expressions is clear. Using the expressions (17)–(20), the effective moduli associated with two matrix Poisson's ratios can be related each other. So, all the numerical calculations are carried out for the matrix

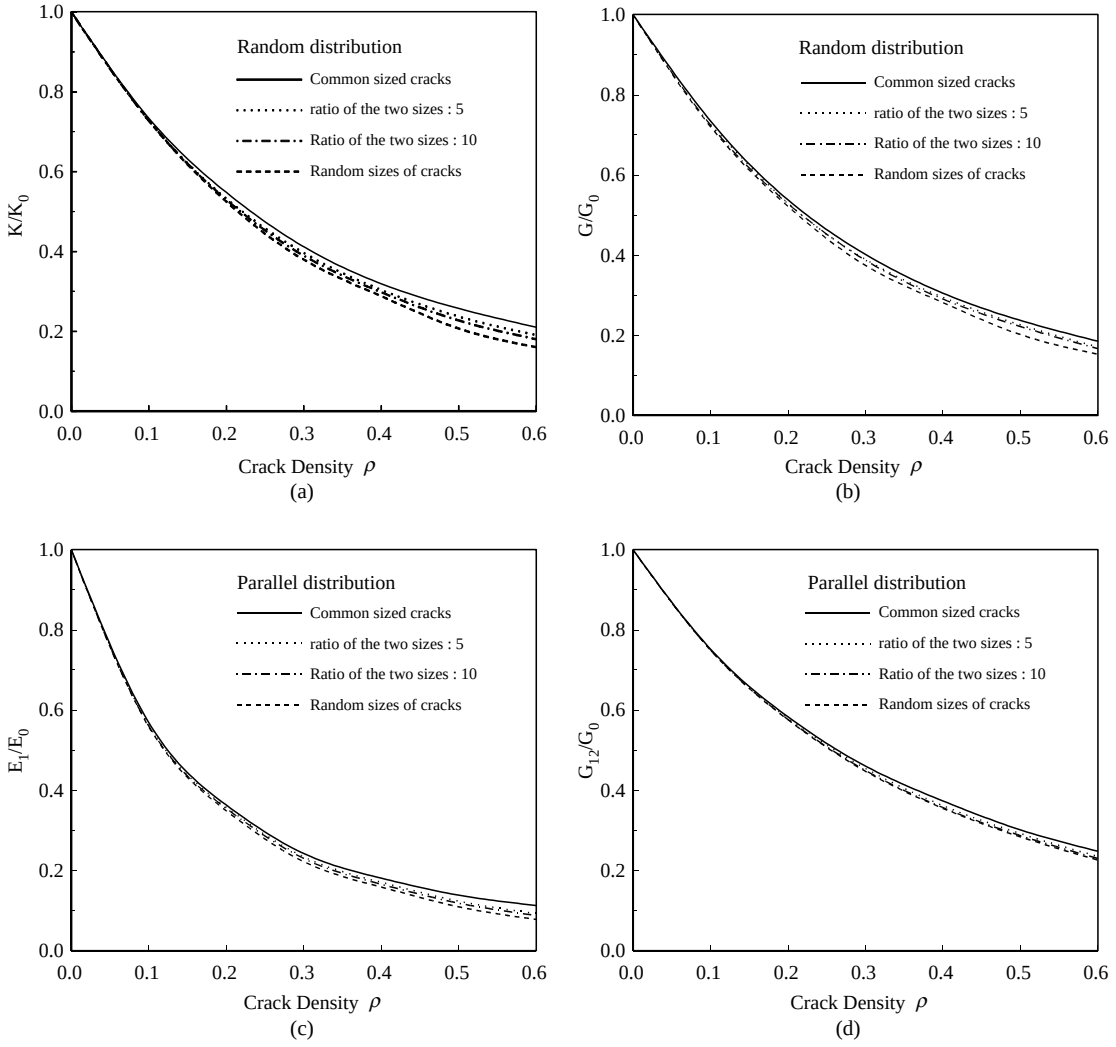

Fig. 10. The effect of crack sizes on the effective moduli for the random and parallel distributions.

Poisson's ratio being 0. The effective moduli with other matrix Poisson's ratio can be correspondingly derived.

5.2. Micromechanics models

Some existing micromechanics models, including the non-interacting solution, the differential method, the generalized non-interacting solution and the generalized self-consistent method are compared with the present numerical results. For convenience, these models are briefly summarized as follows.

For the random and parallel cracks, the non-interacting solutions (e.g., Kachanov, 1992) are

$$\frac{K}{K_0} = 1 \Big/ \left(1 + \frac{\pi\rho}{(1-\nu_0)}\right) \quad \text{and} \quad \frac{G}{G_0} = 1 \Big/ \left(1 + \frac{\pi\rho}{(1+\nu_0)}\right), \tag{21}$$

and

$$\frac{E_1}{E_0} = 1 \Big/ (1 + 2\pi\rho) \quad \text{and} \quad \frac{G_{12}}{G_0} = 1 \Big/ \left(1 + \frac{\pi\rho}{(1+\nu_0)}\right). \tag{22}$$

The differential method for the two types of cracks leads to (e.g., Norris, 1985; Zimmerman, 1985; Hashin, 1988; Huang et al., 1996)

$$\frac{K}{K_0} = 1 \Big/ \left(1 + \frac{1}{(1-\nu_0)}(\mathrm{e}^{\pi\rho} - 1)\right) \quad \text{and} \quad \frac{G}{G_0} = 1 \Big/ \left(1 + \frac{1}{(1+\nu_0)}(\mathrm{e}^{\pi\rho} - 1)\right), \tag{23}$$

and

$$\frac{E_1}{E_0} = 1/(1 + \pi\rho/2)^4 \quad \text{and} \quad \frac{G_{12}}{G_0} = 1 \Big/ \left(1 + \frac{1}{(1+\nu_0)}\left(\pi\rho + \frac{\pi^2}{4}\rho^2\right)\right). \tag{24}$$

It is noticed that (24) are derived from the one associated with a general orthotropic matrix by Hashin (1988), which is a little higher that the closed form solution by Huang et al. (1996). It is also noticed that the plot of Huang et al. (1996) did not follow their closed form solution. However, the plots of the differential method by Zhan et al. (1999) and Feng et al. (2003) seem to follow the closed form solution by Huang et al. (1996).

The generalized self-consistent method for the random cracks gives (Huang et al., 1994)

$$\frac{E}{E_0} = 1 \Big/ (1 + \pi\rho + D_E(\nu_0)\rho^2) \quad \text{and} \quad \frac{G}{G_0} = 1 \Big/ \left(1 + \frac{\pi\rho}{(1+\nu_0)} + D_G(\nu_0)\rho^2\right), \tag{25}$$

where $D_E(\nu_0) = 1.17$, 1.12 and 1.02 and $D_G(\nu_0) = 0.93$, 0.78 and 0.61 for the Poisson's ratio of the matrix being 0.2, 0.3 and 0.4 and the case of plain strain.

Besides, it is worth mentioning the generalized non-interacting solution (Shen and Yi, 2000a, 2001). For the case of 2-D cracks, it gives

$$\frac{K}{K_0} = 1 \Big/ \left(1 + \frac{1}{(1-\nu_0)}\frac{\pi\rho}{1 - \frac{1}{2}\pi\rho}\right) \quad \text{and} \quad \frac{G}{G_0} = 1 \Big/ \left(1 + \frac{1}{(1+\nu_0)}\frac{\pi\rho}{1 - \frac{1}{4}\pi\rho}\right), \tag{26}$$

$$\frac{E_1}{E_0} = 1 \Big/ \left(1 + \frac{2\pi\rho}{1 - \frac{3}{4}\pi\rho}\right) \quad \text{and} \quad \frac{G_{12}}{G_0} = 1 \Big/ \left(1 + \frac{1}{(1+\nu_0)}\frac{\pi\rho}{1 - \frac{1}{4}\pi\rho}\right). \tag{27}$$

It is noticed that Ponte Castañeda and Willis (1995) derived the estimates of Hashin–Shtrikman type, which coincide with the generalized non-interacting solution for general ellipsoidal inhomogeneities by Shen and Yi (2001). For the case of circular or spherical inhomogeneities, the generalized non-interacting solution coincides with the Mori–Tanaka solution. And for the present case of cracks, the generalized non-interacting solution becomes (26) and (27). It is known that the generalized non-interacting solution is derived using the non-interacting approximation to obtain the strain energy change Δf_{micro}. So, it has the same simplicity as the conventional non-interacting solution, while it seems to have rather higher accuracy. The underlying reason causing the difference between the two non-interacting solutions is that the generalized non-interacting solution only neglects the interactions among inhomogeneities, but the conventional one neglect both the interactions among inhomogeneities and the interactions between inhomogeneities and the boundary of a representative sample (see Shen and Yi, 2001). Also, it is noticed some other micromechanics models such as the model by Feng and Yu (2000) and the interactive direct-derivation (IDD) method by Zheng and Du (2001). The model by Feng and Yu (2000) are close to the differential method, and the IDD method by Zheng and Du (2001) coincides with the generalized non-interacting solution when crack density is less than $1/\pi$. In general, all these micromechanics methods are

exact at the first-order according to the Taylor series of crack density, but approximate at the second-order term, as pointed out by many researchers (e.g., Budiansky and O'Connell, 1976; Zimmerman, 1991). So, comparison with the present numerical results may determine which one can provide the optimum estimation of the effective moduli of cracked plates with general crack densities.

5.3. Comparison of micromechanics models, existing and present numerical results

The predictions of micromechanics models (21)–(27), the existing numerical results and the present numerical results for the case of one sized cracks are plotted in Figs. 11 and 12. It is seen from Fig. 11(a)–(d) that the differential method can provide the optimum estimation of the effective moduli of cracked plates with general crack densities though the relative difference is still significant for crack density higher than 0.4. It is noted that the numerical results associated with identical sized cracks are used to compare with the micromechanics models. However, it is seen from the comparison of Figs. 10 and 11 that the numerical

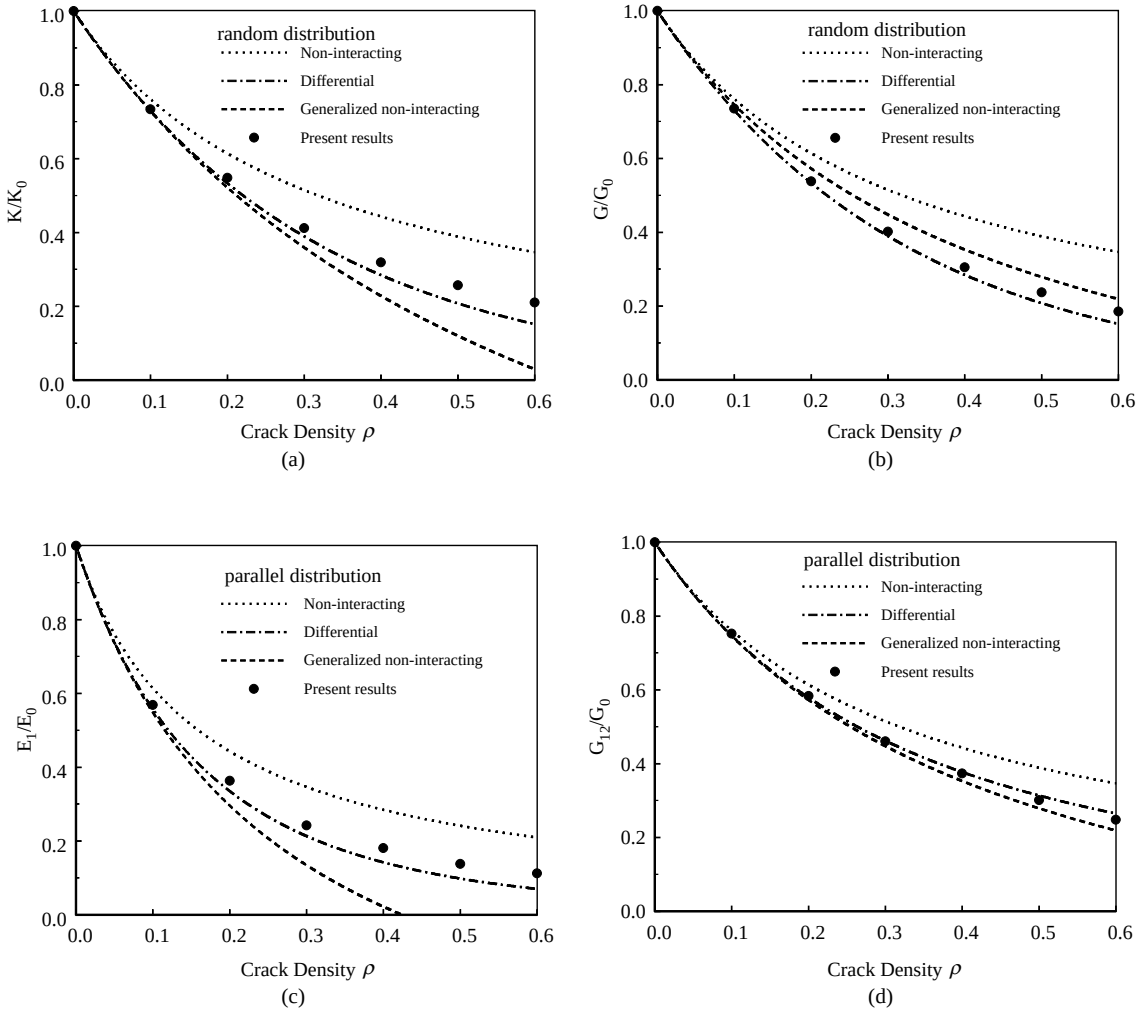

Fig. 11. The comparison of some micromechanics models and the present numerical results associated with one sized cracks.

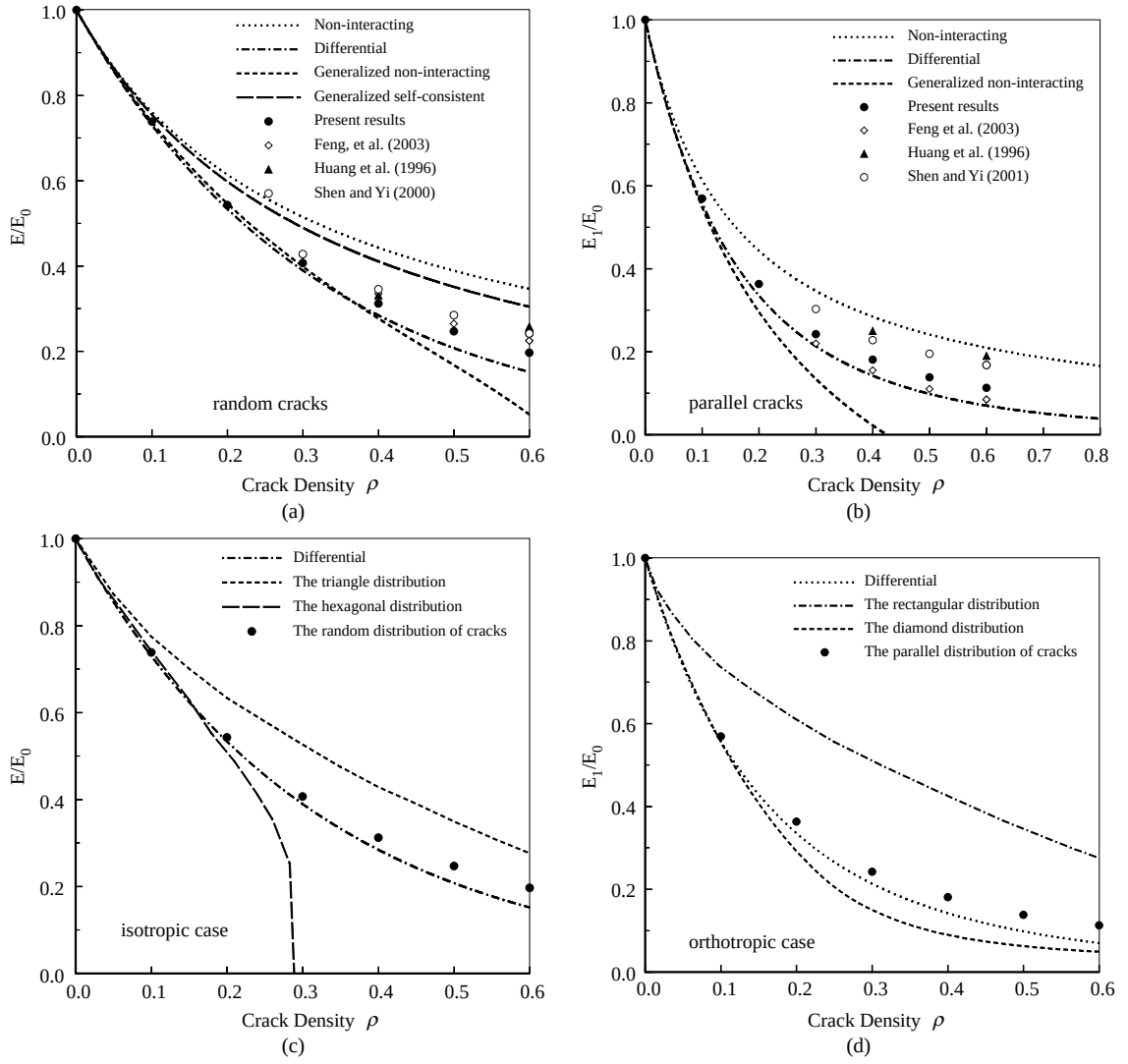

Fig. 12. (a) and (b) For the effective Young's moduli associated with the random and parallel cracks evaluated by various models, (c) and (d) for a comparison of the effective Young's moduli associated with the random and regular distributions of cracks.

results associated with the random sizes of cracks are very close to the predictions of the differential method. The present numerical results about the effect of crack size provide a support to the assertion by Salganik (1973) on the application of the differential method to cracked bodies. He stated that the differential method should be expected to be more accurate as the size distribution becomes broader.

It is noticed that there are no estimations for the parallel cracks using the generalized self-consistent method, and $D_E(\nu_0)$ and $D_G(\nu_0)$ in (25) for the random cracks do not obey the rule of the dependence of effective moduli on the Poisson's ratio described in (17)–(20). Theoretically, $D_E(\nu_0)$ should not depend on the Poisson's ratio, as shown in (19). So the effective Young's modulus based on the generalized self-consistent method is plotted in Fig. 12, where the average value of the three $D_E(\nu_0)$ given by Huang et al. (1994) is assumed.

For the random and parallel cracks, Fig. 12(a) and (b) show the effective Young's moduli predicted by the existing numerical calculations, the present numerical results and the micromechanics models. It is noted that the effective Young's moduli for the random distribution are derived from the corresponding effective bulk and shear moduli when they are not directly given, such as the results by Huang et al. (1996), Shen and Yi (2000b) and the present calculation. When the crack density is lower than 0.3, all the numerical results are close to the predictions of the differential method. So, the numerical results by Renaud et al. (1996) and Zhan et al. (1999) are not plotted in the figures for clarity, as they only analyzed the crack density up to 0.3 and 0.35. However, it is noticed that the results by Zhan et al. (1999) for crack density of 0.35 are significantly larger than the predictions of the differential method. When the crack density becomes larger than 0.3, the differences among these existing numerical results are significant.

It is seen from Fig. 12(a) and (b) that all the numerical results vary between the differential method and the non-interacting solution. It has been mentioned previously that the numerical results of the effective moduli of 2-D cracked solids by Shen and Yi (2000b, 2001) actually involve the approximation of Kachanov's method (Kachanov, 1987). Besides, the sample sizes are also not sufficiently large. Thus, it can be thought that the assumptions and the insufficiently large sample size are the reasons that cause the effective moduli significantly larger than the present ones. Huang et al. (1996) obtained the effective moduli based on unit cells with 25 random or parallel cracks for the crack density up to 0.6. It is seen from Fig. 12(a) and (b) that Huang et al. (1996) are also significantly larger than the present ones. Huang et al. (1996) claimed that the results based on 50 cracks were compared. However, the effect of sample size on the effective moduli in Figs. 6 and 7 shows that when samples are not sufficiently large, the effective moduli tend to become larger for the high crack densities. So it is believed that their sample sizes may not be sufficiently large for the crack densities larger than 0.3. It is also seen from Fig. 12(a) and (b) that the numerical results by Feng et al. (2003) are relatively closer to the present ones. However, it has been checked that Kachanov's method causes the strain energy change Δf_{micro} to become smaller, which causes the effective moduli to become significantly larger. So it is believed that the effect of other approximations involved in the calculations by Feng et al. (2003) may partially cancel with the effect of Kachanov's approximate method.

Fig. 12(c) and (d) shows a comparison between the plates with random and regular cracks. It is interesting to see that when the crack density is lower than 0.15, the effective Young's moduli associated with the random cracks and the hexagonally distributed cracks are agreeable with each other, while the parallel cracks and the cracks with the diamond distribution lead to the similar results. As the two regular distributions of cracks make the Young's moduli of the plates to decay severely, it seems that the amplifying effect of the interaction among randomly distributed cracks is dominant. Actually, as far as the two cases with the crack density being less than 0.15 are considered, the agreement between the generalized non-interacting solution and the present numerical results confirms that the amplifying and shielding effects among randomly distributed cracks on the effective Young's moduli happen to cancel each other. However, the competition of the amplifying and shielding effects of the multiple crack interaction on the effective moduli depends on the far-field stress case, the crack distribution and density. A general and clear conclusion has not been achieved, even though many researchers have considered the problem.

6. Conclusion

An accurate numerical model is proposed to calculate the effective moduli of plates with various distributions and sizes of cracks. The six types of crack distributions and three crack sizes are considered. Some conclusions are summarized as follows.

The comparison with FEM calculations confirms the validity of the proposed numerical model. The calculations for the regular distributions show very interesting results, such as the boundary layer phenomenon and the different effects of the rectangular and diamond distributions on the effective Young's and

shear moduli. For the random and parallel cracks, it is found that when the crack density becomes higher, a larger sample size is required to get stabilized effective moduli, and the sample number 10–20 may be sufficient to get stabilized average values. Among the micromechanics models, the differential method can provide the optimum estimation of the effective moduli. However, the relative differences between the differential method and the present numerical results associated with identically sized cracks are still significant for the crack densities higher than 0.4. But the numerical results associated with the random sizes of cracks are very close to the predictions of the differential method. The effective moduli associated with the regular distributions of cracks may be more sensitive to the crack sizes than those of the random distributions. Also, it is seen that the effective moduli decrease as the size distribution of the cracks gets broader. This provides a support to the assertion by Salganik (1973), who stated that the differential method should be expected to be more accurate as the size distribution becomes broader.

Acknowledgements

This work was supported by National Science Foundation, Surface Engineering and Materials Design program under grant CMS-0305594.

References

Benveniste, Y., 1986. On the Mori–Tanaka's method in cracked bodies. Mech. Res. Commun. 13, 193–201.
Budiansky, B., O'Connell, R.J., 1976. Elastic moduli of a cracked solid. Int. J. Solids Struct. 12, 81–97.
Cherkaev, A.V., Lurie, K.A., Milton, G.W., 1992. Invariant properties of the stress in plane elasticity and equivalence classes of composites. Proc. R. Soc. Lond. Ser. A 438, 519–529.
Christensen, R.M., 1990. A critical evaluation for a class of micromechanics models. J. Mech. Phys. Solids 38, 379–404.
Christensen, R.M., Lo, K.H., 1979. Solutions for effective shear properties in three phase sphere and cylinder models. J. Mech. Phys. Solids 27, 315–330.
Eshelby, J.D., 1957. The determination of the elastic field of an ellipsoidal inclusion and related problems. Proc. R. Soc. Lond. Ser. A 241, 376–396.
Feng, X.-Q., Yu, S.-W., 2000. Estimate of effective elastic moduli with microcracks interaction effects. Theor. Appl. Fract. Mech. 34, 225–233.
Feng, X.-Q., Li, J.-Y., Yu, S.-W., 2003. A simple method for calculating interaction of numerous microcracks and its applications. Int J. Solids Struct. 40, 447–464.
Hashin, Z., 1983. Analysis of composite materials. J. Appl. Mech. 50, 481–505.
Hashin, Z., 1988. The differential method and its application to cracked materials. J. Mech. Phys. Solids 36, 719–734.
Hill, R., 1965. A self-consistent mechanics of composite materials. J. Mech. Phys. Solids 13, 189–198.
Hoenig, A., 1979. Elastic moduli of a non-randomly cracked body. Int. J. Solids Struct. 15, 137–154.
Hu, G.K., Weng, G.J., 2001. A new derivative on the shift property of effective elastic compliance for planar and three-dimensional composites. Proc. R. Soc. Lond. Ser. A 457, 1675–1684.
Huang, Y., Hu, K.X., Chandra, A., 1994. A generalized self-consistent mechanics method for microcracked solids. J. Mech. Phys. Solids 42, 1273–1291.
Huang, Y., Chandra, A., Jiang, Z.Q., Wei, X., Hu, K.X., 1996. The numerical calculation of two-dimensional effective moduli for microcracked solids. Int. J. Solids Struct. 33, 1575–1586.
Ju, J.W., Chen, T.M., 1994. Micromechanics and effective moduli of elastic composites containing randomly dispersed ellipsoidal inhomogeneities. Acta Mech. 103, 103–121.
Kachanov, M., 1987. Elastic solids with many cracks: a simple method of analysis. Int. J. Solids Struct. 23, 23–43.
Kachanov, M., 1992. Effective elastic properties of cracked solids: critical review of some basic concepts. Appl. Mech. Rev. 45, 304–335.
Kachanov, M., 1994. Elastic solids with many cracks and related problems. Adv. Appl. Mech. 30, 259–445.
Laws, N., Brockenbrough, J.R., 1987. The effect of microcrack systems on loss of stiffness of brittle solids. Int. J. Solids. Struct. 23, 1247–1268.

Laws, N., Dvorak, G.J., 1987. The effect of fiber breaks and aligned penny-shaped cracks on the stiffness and energy release rates in unidirectional composites. Int. J. Solids Struct. 23, 1269–1283.

Mori, T., Tanaka, K., 1973. Average stress in matrix and average elastic energy of materials with misfitting inclusions. Acta Metall. 21, 571–574.

Muskhelishvili, N.I., 1963. Some Basic Problems of the Theory of Elasticity. Noordhoff, Groningen.

Nemat-Nasser, S., Hori, M., 1993. Micromechanics: Overall Properties of Heterogeneous Materials. Elsevier, Amsterdam.

Nemat-Nasser, S., Hori, M., 1995. Universal bounds for overall properties of linear and nonlinear heterogeneous solids. J. Eng. Mater. Technol. 117, 412–432.

Nemat-Nasser, S., Yu, N., 1993. Solids with periodically distributed cracks. Int. J. Solids Struct. 30, 2071–2095.

Norris, A.N., 1985. A differential method for the effective moduli of composites. Mech. Mater. 4, 1–16.

Ponte Castañeda, P., Willis, J.R., 1995. The effect of spatial distribution on the effective behavior of composite materials and cracked media. J. Mech. Phys. Solids 43, 1919–1951.

Renaud, V., Kondo, D., Henry, J.P., 1996. Computations of effective moduli for microcracked materials: a boundary element approach. Comput. Mater. Sci. 5, 227–237.

Salganik, R.L., 1973. Mechanics of bodies with many cracks. Mech. Solids 8, 135–143.

Shen, L., Yi, S., 2000a. New solutions for effective elastic moduli of microcracked solids. Int. J. Solids Struct. 37, 3525–3534.

Shen, L., Yi, S., 2000b. Approximate evaluation for effective elastic moduli of cracked solids. Int. J. Fract. 106, L15–L20.

Shen, L., Yi, S., 2001. An effective inclusion model for effective moduli of heterogeneous materials with ellipsoidal inhomogeneities. Int. J. Solids Struct. 38, 5789–5805.

Weng, G.J., 1984. Some elastic properties of reinforced solids, with special reference to isotropic ones containing spherical inclusions. Int. J. Eng. Sci. 22, 845–856.

Weng, G.J., 1990. The theoretical connection between Mori–Tanaka's theory and the Hashin–Shtrikman–Walpole bounds. Int. J. Eng. Sci. 28, 1111–1120.

Willis, J.R., 1981. Variational and related methods for the overall properties of composites. Adv. Appl. Mech. 21, 1–78.

Zhan, S., Wang, T., Han, X., 1999. Analysis of two-dimensional finite solids with microcracks. Int. J. Solids Struct. 36, 3735–3753.

Zheng, Q.-S., Hwang, K.C., 1996. Reduced dependence of defect compliance on matrix and inclusion elastic properties in two-dimensional elasticity. Proc. R. Soc. Lond. A 452, 2493–2507.

Zheng, Q.-S., Du, D.-X., 2001. An explicit and universally applicable estimate for the effective properties of multiphase composites which accounts for inclusion distribution. J. Mech. Phys. Solids 49, 2765–2788.

Zimmerman, R.W., 1985. The effect of microcracks on the elastic moduli of brittle materials. J. Mater. Sci. Lett. 4, 1457–1460.

Zimmerman, R.W., 1991. Elastic moduli of a solid containing spherical inclusions. Mech. Mater. 12, 17–24.